for these energies, especially in the case of V^{51} and Co^{59}. Only the proton spectra will establish whether the percentage of the (p,p') cross section due to direct interaction is large enough that, when subtracted from the total (p,p') cross section, it will fit with the calculations done for $r_0=1.5$ F, or if the inverse-reaction cross section was larger due to a lower Coulomb barrier for the excited nuclei.

ACKNOWLEDGMENTS

Our thanks go to Dr. J. Anderson and Dr. J. Benveniste for stimulating discussions and for permitting us to use experimental data previous to publication. We also thank Henry Catron, D. R. Rawles, and the crew of the 90-in. cyclotron for their cooperation during the running of the experiment, and Don Freedman who wrote the IBM programs.

PHYSICAL REVIEW VOLUME 128, NUMBER 1 OCTOBER 1, 1962

Level Structure in Ne^{22} and Si^{30} from the Reactions $O^{18}(\alpha,n)Ne^{21}$ and $Mg^{26}(\alpha,n)Si^{29}$

J. K. Bair and H. B. Willard
Oak Ridge National Laboratory, Oak Ridge, Tennessee

(Received April 6, 1962; revised manuscript received June 20, 1962)

Compound states of high excitation in Ne^{22} and Si^{30} have been observed in the total neutron yield from the reaction $O^{18}(\alpha,n)Ne^{21}$ and $Mg^{26}(\alpha,n)Si^{29}$. In the case of Ne^{22}, twenty-five resonances were observed, varying in width from 5 to 150 keV for alpha bombarding energies from 2.5 to 5 MeV (excitation energy from 11.7 to 13.8 MeV). The reaction $Mg^{26}(\alpha,n)Si^{29}$ showed forty resonances varying in width from less than 10 to 60 keV for alpha energies from 3 to 5.3 MeV (excitation energy from 13.3 to 15.3 MeV). Absolute cross sections were measured for both reactions. A statistical analysis of the area under the excitation curves gives an alpha-particle strength function $\bar{S}_\alpha=0.02_6$ for $O^{18}+\alpha$ and $\bar{S}_\alpha=0.01_6$ for $Mg^{26}+\alpha$. Analysis of the individual resonances in $O^{18}+\alpha$ gives a value of $\langle\gamma_\alpha^2\rangle/D\leq 0.04$, in agreement with the $\bar{S}_\alpha$ obtained by the statistical analysis. The strength functions are probably reliable to better than a factor of 2.

INTRODUCTION

COMPOUND states of high excitation in Ne^{22} have been studied by means of the reaction $O^{18}(\alpha,n)Ne^{21}$ by Roy *et al.*[1] using natural alpha particles, and by Bonner *et al.*[2] using accelerated particles. Roy's experiments suffered from the inherent lack of resolution typical of natural alpha sources. The work of the Rice group showed much structure; however, due to the target thickness (120 keV for 2-MeV alphas), most of the resonances were unresolved. Several investigators[3] have studied the $Mg^{26}(\alpha,n)Si^{29}$ reaction using natural alpha sources with poor energy resolution. No other experiments have been reported covering these high high excitation energies in the compound nuclei.

EXPERIMENTAL PROCEDURES

The $(He^4)^+$ beam of the ORNL 5.5-MV Van de Graaff was stripped to $(He^4)^{++}$ before entering the 90° analyzing magnet. After bending and energy analysis, it was allowed to bombard thin targets of high isotopic purity placed at the center of the graphite-sphere neutron detector.[4] Detector efficiency was checked with a radium-beryllium neutron source which had been calibrated by comparison with a Bureau of Standards source. For the neutron energies obtained here the response of the ball[4] is constant to within less than $\pm 5\%$. Bombarding alpha energies were determined by calibrating the magnet with the $Li^7(p,n)Be^7$ reaction, utilizing the known proton calibration, and correcting the calibration constant with the known ratio of alpha-to-proton mass. It is estimated that the energy calibration is accurate to $\pm 0.2\%$. Narrow resonances measured with several targets at various times repeated to within this figure.[5]

$O^{18}(\alpha,n)Ne^{21}$

The O^{18} targets used for the yield curves were prepared by anodizing tantalum blanks in water[6] whose oxygen was enriched to greater than 97% O^{18}. Since target thickness is proportional to the anodizing voltage, a series of targets could easily be prepared with reasonably well-known ratios of thicknesses. The thinnest target had a small energy loss compared to the narrowest resonance and the natural widths thus

[1] R. R. Roy, A. Lagasse, M. Goes, and R. Moerman, Compt. Rend. **241**, 1567 (1955).
[2] T. W. Bonner, A. A. Kraus, Jr., J. B. Marion, and J. P. Schiffer, Phys. Rev. **102**, 1348 (1956).
[3] A. Meye, Z. Physik **105**, 232 (1937); I. Halpern, Phys. Rev. **76**, 248 (1949); J. Nagy, Acta Phys. Acad. Sci. Hung. **3**, 14 (1953); E. Csongor, Nuclear Phys. **23**, 107 (1961).
[4] R. L. Macklin, Nuclear Instr. **1**, 335 (1957).
[5] It is interesting to note that during the course of this work the $B^{10}(\alpha,n)$ resonance at about 1.5 MeV, measured as a calibration check point, consistently indicated that the current best value of 1.518 MeV is about 0.7% high.
[6] Obtained from the Weizmann Institute.

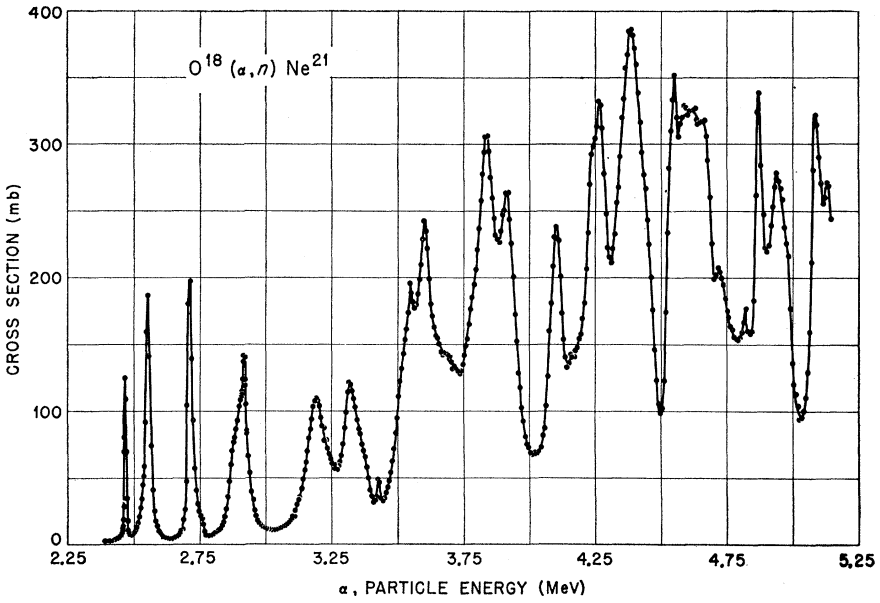

FIG. 1. The neutron yield curve as obtained using an O^{18} target, 6-keV thick for 2.5-MeV α particles.

measured agreed with those calculated knowing the ratio of the thickness of other targets. Figure 1 shows the yield of neutrons obtained with a target 6-keV thick for 2.5-MeV α particles. Figure 2 shows the lowest four resonances measured with a target whose thickness was less than 2 keV.

The absolute cross sections shown on Fig. 1 were obtained using a gas target enriched to greater than 97% O^{18}.[6] Using this target at several gas pressures, the yield over the two resonances near 3.25 MeV was measured. The largest error in the cross section given is believed to be the correction for finite energy resolution of the gas target. Our value for the cross section

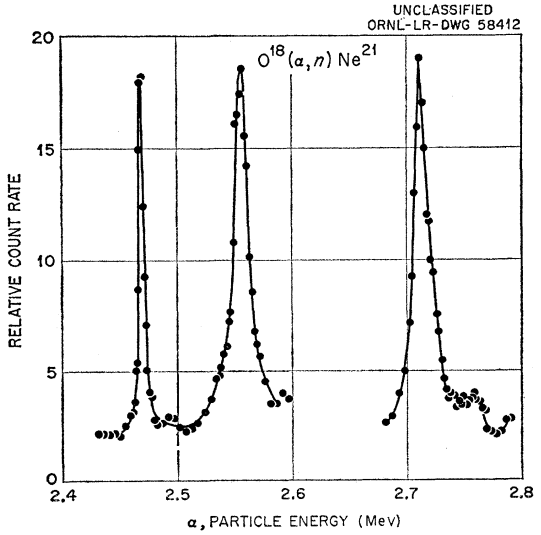

FIG. 2. The $O^{18}(\alpha,n)Ne^{21}$ yield at the lowest four resonances measured with a target less than 2-keV thick for 2.5-MeV α particles.

at the peak of the 3.19-MeV resonance is 109 ± 25 mb. Table I lists the resonant α energies, estimates of the experimental widths, and excitation energies in Ne^{22} (based on $O^{18}+\alpha-Ne^{21}=9.667$ MeV).

$Mg^{26}(\alpha,n)Si^{29}$

A series of magnesium targets of various thicknesses was prepared by evaporating enriched MgO(99% Mg^{26}) from a tantalum boat onto tantalum backings. Since the ratio of MgO to Mg was not known or controlled, no attempt was made to obtain target thicknesses by weighing; instead suitable regions of the yield curve were run with targets of successively less magnesium area density until the shape of the narrowest resolved level remained unchanged. Figure 3 shows a typical yield curve taken with a sufficiently thin target. The background, shown by the triangles, was taken with the target replaced by clean tantalum. Separate targets[7] with carefully weighed amounts of material were used to obtain the cross section. The error in the cross section probably is $+25\%-50\%$ with the largest uncertainty being in the ratio of MgO to Mg. Table II lists the resonant α energies, estimates of the experimental widths, and excitation energies in Si^{30} (based on $Mg^{26}+\alpha-Si^{30}=10.616$ MeV).

DISCUSSION

Table I gives the pertinent parameters of the level structure of Ne^{22} as obtained from this work. Column 5 gives the value of $4\pi\lambda^2$ times the maximum possible value of $\Gamma_\alpha\Gamma_n/\Gamma^2$, i.e., 1/4. Thus, the minimum possible

[7] Kindly prepared by the group at ORNL under the direction of B. J. Massey.

TABLE I. The level parameters for $O^{18}+\alpha$: Columns 2, 3, and 4 give, respectively, the resonant α energy, the energy of excitation in the compound Ne^{22} nucleus, and the experimental width. Column 5 gives the value of $4\pi\lambda^2$ times the maximum possible value of $\Gamma_\alpha\Gamma_n/\Gamma^2$, i.e., 1/4. Column 6 shows that spin zero seems to be ruled out for many of the levels by the considerations of column 5. Columns 7, 8, 9, 10, and 11 give estimates of the dimensionless reduced widths.

Level	E_R (MeV)	E_X (MeV)	Γ_{exp} (keV)	$4\pi\lambda^2/4$ (mb)	J_{min}	Θ_0^2 (%)	Θ_1^2 (%)	Θ_2^2 (%)	Θ_3^2 (%)	Θ_4^2 (%)
1	2.468±0.010	11.686	5	100	$J>0$	3.6	6.1	15	61	340
2	2.556±0.010	11.758	14	96	$J>0$	7.9	12.7	29	120	700
3	2.711±0.010	11.885	13	90	$J>0$	4.6	7.5	18	66	360
4	2.75	11.92	30±15	89		9.2	15.3	36	130	710
5	2.90	12.04	70	85	$J>0$	15	24.8	57	210	1100
6	2.919±0.010	12.055	10	84		2.1	3.5	8.1	30	150
7	3.19	12.28	80	76	$J>0$	9.0	14.7	31	110	480
8	3.32	12.38	80	75	$J>0$	8.9	14.5	31	110	470
9	3.43	12.47	15	72		1.2	1.8	4.3	12	49
10	3.55	12.57	≈20	70		≈1.6	≈2.4	≈ 4.8	≈14	≈57
11	3.60	12.61	30	68	$J>0$	2.2	3.2	6.5	19	82
12	3.84	12.81	45	64	$J>0$	2.6	3.8	6.9	19	69
13	3.92	12.87	45	63	$J>0$	2.5	3.6	6.3	16	63
14	4.10	13.02	50	60	$J>0$	2.5	3.3	6.0	14	47
15	4.24	13.14	≈30	58		≈1.4	≈1.9	≈ 3.0	≈ 6.8	≈22
16	4.27	13.16	≈30	57	$J>0$	≈1.4	≈1.9	≈ 3.0	≈ 6.8	≈22
17	4.39	13.26	100	56	$J>0$	4.3	5.4	8.6	18	57
18	4.52	13.36	≈20	54	$J>0$	≈0.9	≈1.1	≈ 1.6	≈ 3.2	≈ 8.9
19	4.60	13.43	≈150	54	$J>0$	≈6.0	≈7.3	≈11	≈21	≈62
20	4.67	13.48	≈20	52		≈0.8	≈1.0	≈ 1.3	≈ 2.7	≈ 7.3
21	4.72	13.53	≈20	52		≈0.8	≈1.0	≈ 1.3	≈ 2.7	≈ 7.3
22	4.82	13.61	≤10	51		≤0.3	≤0.4	≤ 0.5	≤ 1.0	≤ 2.7
23	4.87	13.65	25	51	$J>0$	0.9	1.1	1.4	2.7	6.9
24	4.95	13.72	80	50	$J>0$	2.9	3.4	4.2	7.7	20
25	5.09	13.83	30	49	$J>0$	1.1	1.2	1.5	2.6	6.4

value of $2J+1$, where J is the spin of the compound level, is given by the measured cross section divided by the figure given in column 5. As shown in column 6, these considerations seem to rule out spin-zero states for most of the levels. The spin of the ground state of the residual Ne^{21} nucleus is $3/2^+$, that of the first excited state is $3/2^+$ or $5/2^+$, and that of the second excited state is unknown. Assuming that the neutron emission is limited to the ground and first excited states, then compound states of 0^+ would require a minimum $l_n=2$, where as a 1^- or a 2^+ state could decay by $l_n=1$ and $l_n=0$ neutrons, respectively. (Only the natural parity states are involved since we are bombarding a 0^+ ground state with alpha particles.) Thus, the neutron penetrabilities tend to suppress compound states of spin zero in general agreement with the above interpretation of the data. The statistical factor $(2J+1)^{-1}$ for the level spacing would also tend to reduce the number of $J=0$ levels.

Columns 7, 8, 9, 10, and 11 give the dimensionless reduced widths

$$\Theta_l^2=\frac{\gamma_l^2}{\frac{3}{2}\hbar^2/\mu R} \quad \text{with} \quad \gamma_l^2=\frac{\Gamma}{2kv_l},$$

where the reaction radius was taken to be

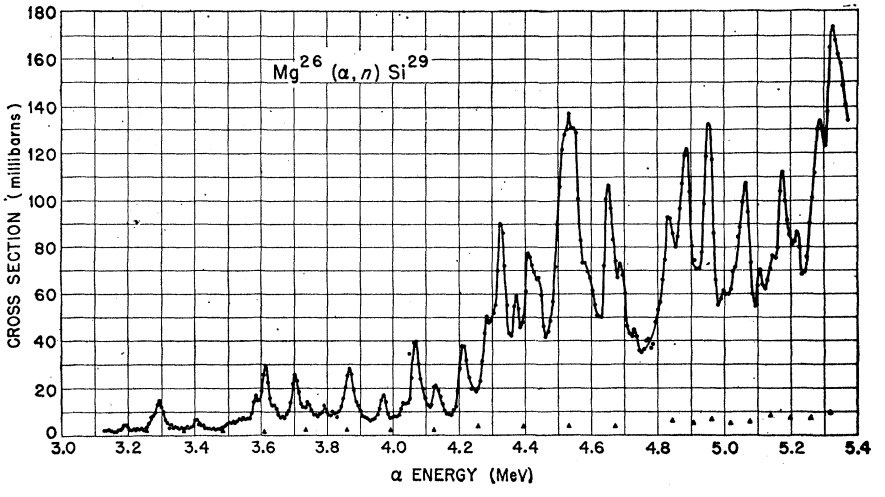

FIG. 3. The $Mg^{26}(\alpha,n)Si^{29}$ thin-target yield curve. The triangles represent the tantalum background.

TABLE II. The resonant α energies, experimental widths, and excitation energies in the compound Si^{30} nucleus are given, as determined by the reaction $Mg^{26}(\alpha,n)Si^{29}$.

Resonance	E (MeV)	Γ_{exp} (keV)	E_X (MeV)	Resonance	E (MeV)	Γ_{exp} (keV)	E_X (MeV)
1	3.19	20	13.38	21	4.44	25	14.46
2	3.27	···	13.45	22	4.53	60	14.54
3	3.29	30	13.47	23	4.53	<10	14.54
4	3.40	20	13.56	24	4.58	···	14.58
5	3.58	≈10	13.72	25	4.65	25	14.65
6	3.61	30	13.74	26	4.69	15	14.68
7	3.64	···	13.77	27	4.73	···	14.71
8	3.70	30	13.82	28	4.83	20	14.80
9	3.74	15	13.86	29	4.89	25	14.85
10	3.79	15	13.90	30	4.95	25	14.91
11	3.87	30	13.97	31	4.99	···	14.94
12	3.97	20	14.06	32	5.03	···	14.97
13	4.03	···	14.11	33	5.07	30	15.01
14	4.07	25	14.14	34	5.11	15	15.04
15	4.13	20	14.19	35	5.14	···	15.07
16	4.21	25	14.26	36	5.18	20	15.10
17	4.28	···	14.32	37	5.22	15	15.14
18	4.33	20	14.37	38	5.28	20	15.19
19	4.37	15	14.40	39	5.32	25	15.23
20	4.41	25	14.44				

$1.45(A^{1/3}+1.59)\times10^{-13}$ cms. Since the Γ used in the calculations was the total width and the ν_l, the penetrability for α particles, the value Θ_l^2 will in general be overestimated; however they are an indication of the maximum probable J values.

Figures 4 and 5 show plots of the logarithm of the number of levels having a level spacing greater than the spacing D. If the distribution is random, these plots should give a straight line whose slope is simply related to the average level spacing. The intercept on the log$N$ axis should correspond to the total number of levels.

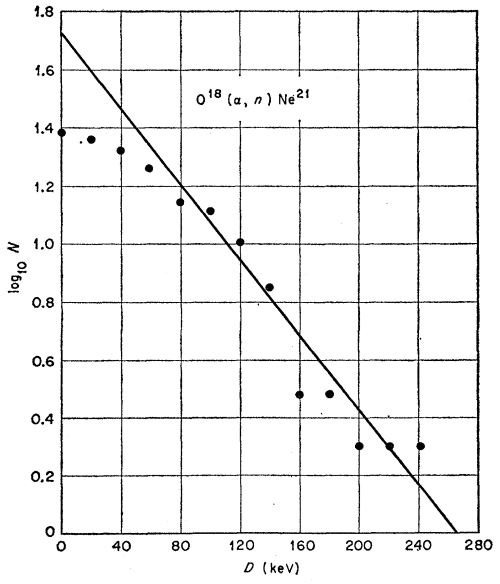

FIG. 4. Plot of the log of the number of levels in $O^{18}(\alpha,n)Ne^{21}$ having a spacing greater than some spacing D. The intercept corresponds to a total of 54 levels of which we observe 25. The slope corresponds to a level spacing of 67 keV.

In the case of $O^{18}+\alpha$, the data show considerable deviation from a straight line for level spacings of less than 40 or 60 keV. Such deviations may occur if the experimental resolution is sufficiently poor to cause narrow resonances to be missed, if there is overlap of the levels, or if for some reason the distribution

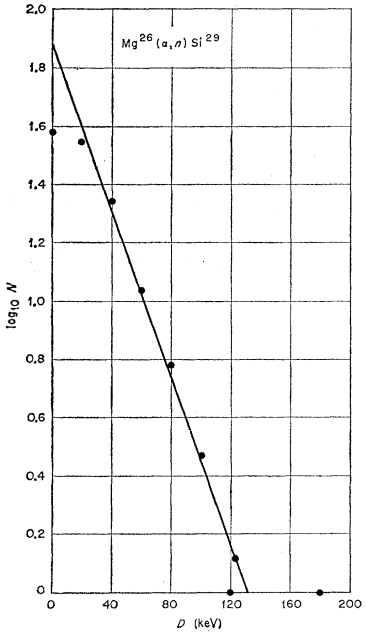

FIG. 5. Plot of the log of the number of levels in $Mg^{26}(\alpha,n)Si^{29}$ having a spacing greater than some spacing D. The intercept corresponds to a total of 73 levels of which we observe 40. The slope corresponds to a level spacing of 30 keV.

is not random, or, of course, if the sample is too small. In the present case, the experimental resolution is certainly much better than 40 keV, and can not be blamed for the deviation. If there is overlap of levels, then the average level spacing of 67 keV obtained from the slope of the straight line should be an upper

limit. The intercept corresponds to a total number of levels $N_0=54$ within the energy range covered, thus giving an average spacing of about 51 keV in agreement with the previous value of 67 keV considered to be an upper limit only. No explanation for the deviation of the data from the straight line is offered. The spacing of $J=0$ levels, under the assumption that the level spacing varies by $(2J+1)^{-1}$ and that $J_{\max}\leq 3$, is approximately one MeV.

In the case of $Mg^{26}+\alpha$, the points do fall rather well on the straight line shown whose slope corresponds to an average spacing of 30 keV. The intercept corresponds to a total number of levels $N_0=73$ of which we actually observe about 40. The fact that the points deviate from the straight line below 20 keV indicates that the over-all resolution is at least this good. The average spacing of 31 keV obtained from the extrapolated N_0 and the energy range covered is in excellent agreement with that obtained from the slope. For this case, under the assumption used above, the spacing of $J=0$ levels is approximately 500 keV.

Following the analysis used by Schiffer and Lee[8] and Clarke, Almqvist, and Paul,[9] we have averaged the cross-section data over an energy ΔE and plotted the area under the yield curve per unit ΔE as a function of the incident α-particle energy. These data are shown in Figs. 6 and 7. In the case of O^{18} the ΔE used was 500 keV, and in the case of Mg^{26} a ΔE of 400 keV was used. Under the assumption that $\Gamma_n\gg\Gamma_\alpha$ and that all other widths are negligible [the (α,p) reaction in O^{18} has $Q=-5.6$ MeV and Mg^{26} has $Q=-2.9$ MeV], a value of the α-particle strength function, $\bar{S}_\alpha$, was obtained for each data point shown, from the expression

$$\frac{A_{\Delta E}}{\Delta E}=2\pi^2\lambda\!\!\!^{-2}\left[\sum_l(2l+1)\frac{2kR}{A_l^2}\right]\bar{S}_\alpha.$$

Here, $A_{\Delta E}/\Delta E$ is the unit area under the averaged yield curve and the other symbols have their usual meanings. This formula is based on the assumption that the effect of any interference in the total cross section is zero when averaged and that a simple sum of single level Breit-Wigner terms may be used. These $\bar{S}_\alpha$ as a function of E_α were within $\pm 50\%$ of their averages for both O^{18} and Mg^{26}. The average values $\bar{S}_\alpha$ so obtained were 0.02_6 for $O^{18}+\alpha$, and 0.01_6 for $Mg^{26}+\alpha$, and are probably reliable to better than a factor of two.

For the reaction $O^{18}+\alpha$ where the levels are well enough resolved to be able to obtain reasonably good values of the widths and cross sections, it is possible to make an individual resonance analysis and obtain an average reduced width which can be compared to the strength functions obtained from the analysis discussed above. Table III lists, for the individual levels in $O^{18}+\alpha$, values of $\sigma\Gamma/4\pi\lambda\!\!\!^{-2}=(2J+1)\Gamma_\alpha$ (column 4) for the assumption $\Gamma_n\gg\Gamma_\alpha$. If in addition one makes the assumption that $J=1$ for all the levels, one can calculate the α-particle widths, the reduced widths, and the dimensionless reduced widths, which are tabulated in columns 5, 6, and 7. The average of the reduced widths, $\langle\gamma_{\alpha(J=1)}{}^2\rangle$, is 4.3 keV, and the averaged dimen-

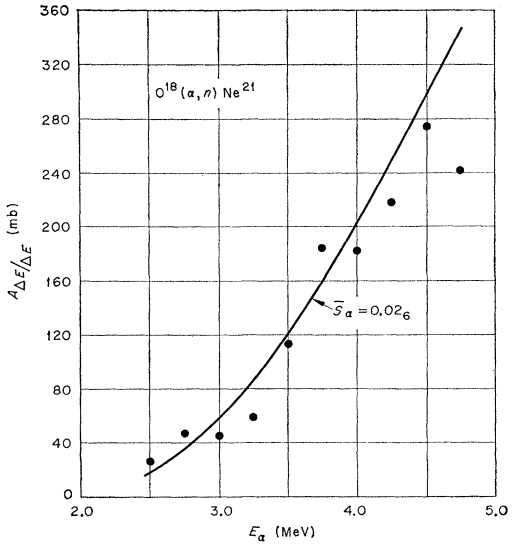

FIG. 6. Plot of $A_{\Delta E}/\Delta E$ as a function of incident α-particle energy for the reaction $O^{18}(\alpha,n)Ne^{21}$. Here $A_{\Delta E}$ is the area under the excitation curve in some energy region ΔE. The solid curve is the calculated curve based on an α-particle strength function $\bar{S}_\alpha=0.02_6$.

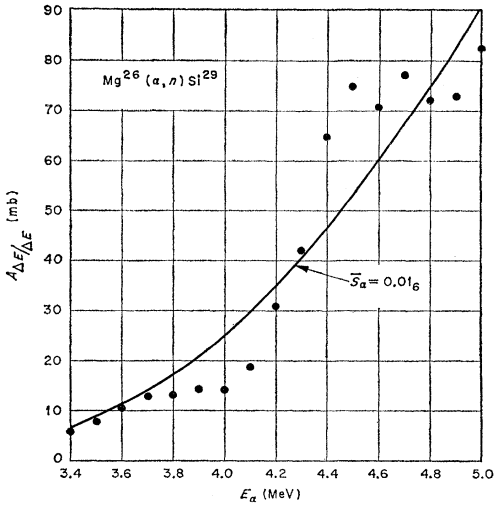

FIG. 7. Plot of $A_{\Delta E}/\Delta E$ as a function of incident α-particle energy for the reaction $Mg^{26}(\alpha,n)Si^{29}$. Here $A_{\Delta E}$ is the area under the excitation curve in some energy region ΔE. The solid curve is the calculated curve based on an α-particle strength function $\bar{S}_\alpha=0.01_6$.

[8] J. P. Schiffer, L. L. Lee, R. H. Davis, and F. W. Prosser, Jr., Phys. Rev. **107**, 547 (1957); J. P. Schiffer and L. L. Lee, Phys. Rev. **107**, 640 (1957); **109**, 2098 (1958).

[9] R. L. Clarke, E. Almqvist, and E. B. Paul, Nuclear Phys. **14**, 472 (1959/60).

TABLE III. The level parameters for $O^{18}+\alpha$: Column 4 lists values of $(\alpha\Gamma/4\pi\lambda^2)=(2J+1)\Gamma_\alpha$ for the assumption $\Gamma_n\gg\Gamma_\alpha$. Column 5 lists the Γ_α for the additional assumption of $J=1$. Columns 6 and 7 tabulate the corresponding reduced widths and dimensionless reduced widths.

Resonance	E_α (MeV)	Γ (keV)	$\sigma\Gamma/4\pi\lambda^2$ (keV)	$\Gamma_{\alpha(J=1)}$ (keV)	γ_1^2 (10^{-13} keV-cm)	Θ_1^2 (%)
1	2.468	5	1.6	0.54	26	0.8
2	2.556	14	6.7	2.2	72	2.3
3	2.711	13	7.1	2.4	52	1.7
4	2.75	30±15	2.1	0.71	14	0.5
5	2.90	70	18	5.9	80	2.5
6	2.919	10	1.5	0.5	9.4	0.3
7	3.19	80	26	8.7	62	2.0
8	3.32	80	27	8.9	62	2.0
9	3.43	15	≈ 1.3	≈ 0.44	≈ 2.1	≈0.1
10	3.55	≈20	≈ 5.0	≈ 1.7	≈ 7.8	≈0.2
11	3.60	30	11	3.7	15	0.5
12	3.84	45	18	5.9	19	0.6
13	3.92	45	≈ 18	≈ 6.0	≈18	≈0.6
14	4.10	50	31	10	27	0.9
15	4.24	≈30	≈ 6.5	≈ 2.2	≈ 4.7	≈0.1
16	4.27	≈30	≈ 13	≈ 4.4	≈10	0.3
17	4.39	100	≈ 79	≈26	≈55	≈1.7
18	4.52	≈20	≈ 9.3	≈ 3.1	≈ 6.2	≈0.2
19	4.60	≈150	≈100	≈35	≈65	≈2.0
20	4.67	≈20	≈ 9.6	≈ 3.2	≈ 5.7	≈0.2
21	4.72	≈20	≈ 4.8	≈ 1.6	≈ 2.9	≈0.1
22	4.82	≲10	≲ 2.5	≲ 0.83	≲ 1.4	0.0
23	4.87	25	19	6.2	10	0.3
24	4.95	80	40	13	22	0.7
25	5.09	30	16	5.2	7.8	0.2

sionless reduced width is 0.8% of the Wigner limit. The assumption of $J=1$ is not, in this particular case, critical; if the assumption $J=2$ were made, the resulting $\langle\gamma_{\alpha(J=2)}{}^2\rangle$ would be 3.7 keV. If one divides these values by the experimental average level spacing of about 100 keV, an upper limit of 0.04 is obtained for the strength function. The spacing of $J=0$ levels has been seen to be about one Mev. Under the same assumptions the spacing for $J=1$ levels is about 1/3 MeV and that for $J=2$ levels is about 1/5 MeV. These values, with the average reduced widths given above, yield estimates for $\bar{S}_{\alpha(J=1)}=0.01_3$ and $\bar{S}_{\alpha(J=2)}=0.01_9$.